Geomechanics and Engineering, *Vol. 26, No. 6 (2021) 581-591*
https://doi.org/10.12989/gae.2021.26.6.581

Nonlinear creep damage model of rock salt considering temperature effect and its implement in FLAC^{3D}

Tianzhu Huang[1,2], Jianlin LI[1,2] and Baoyun Zhao *[3,4]

[1]*College of Civil Engineering and Architecture, China Three Gorges University, Yichang City, Hubei Province, 443002, China*
[2]*Key Laboratory of Geological Hazards on Three Gorges Reservoir Area of Ministry of Education, China Three Gorges University, Yichang City, Hubei Province, 443002, China*
[3]*Graduate Office, Chongqing University of Science and Technology, Chongqing, 401331, China*
[4]*School of Civil Engineering and Architecture, Chongqing University of Science and Technology, Chongqing, 401331, China*

(Received June 1, 2021, Revised August 14, 2021, Accepted September 27, 2021)

Abstract. Laboratory tests were carried out to study the effect of temperature on the long-term strength of rock salt, the creep modulus was defined and the evolution equation of creep thermal damage of rock salt was established. Based on the creep test results of rock salt, a nonlinear thermal visco-plastic damage model considering the influence of temperature damage and expressing the accelerated creep behavior of rock salt is established. According to the construction method of nonlinear creep model, a new nonlinear visco-elastic-plastic creep damage model considering the influence of temperature (nonlinear T-VEPD creep model) is established by concatenating the nonlinear thermal visco-plastic damage model with the Burgers creep model. And then the parameter inversion identification of the model, the results show that the model can well describe the creep properties of rock salt. The finite difference expression of nonlinear T-VEPD creep model is derived by using finite difference theory. The dynamic link calculation program (.dll) of the model is obtained by using the programming and FLAC^{3D} secondary development interface, and then the creep model is verified by laboratory test simulation.

Keywords: creep; damage; nonlinear creep model; rock salt

1. Introduction

Underground caverns in rock salt have been widely used to reserve energy such as natural gas (Obst 2019). The underground burial depth of the rock salt gas storage is generally below 500m. The surrounding rock of the gas storage is affected by the geostress and will be affected by the formation temperature. During the operation phase of the gas storage, it will be affected by the interaction of temperature, ground stress and storage gas pressure for a long time (Khaledi *et al*. 2016, Shkuratnik *et al*. 2019). Therefore, in order to ensure the safe operation of the gas storage, it is necessary to study the creep properties and deformation of rock salt under the combined action of temperature, stress and time. The creep constitutive model of rock can accurately reflect the internal law and deformation mechanism of rock creep. Therefore, the establishment of creep model and the identification of its parameters are an important part of the study of gas storage stability.

The research on creep model theory started earlier (Haupt 1991, Leoni *et al*. 2008). Various creep models have been proposed, mainly including empirical models and element combination models. The empirical model is an empirical relationship fitted by creep test data, mainly the expression of some relationship in stress, strain, creep rate and time (Gray and Whittaker 2015). The element combination model is composed of basic element (elasticity, viscosity and plasticity) by series, parallel and hybrid (Fahimifar *et al*. 2010, Sharifzadeh *et al*. 2013). The element combination model is widely used because its concept is very intuitive and simple, and can fully reflect the creep properties of rock. However, since the basic elements are linear, the model composed of many linear elements still cannot accurately describe and reflect the nonlinear characteristics of the rock. Many scholars (Lyakhovsky *et al*. 2011, Nazary *et al*. 2015, Pestrenin and Pestrenina 2010) have gradually studied the nonlinear creep model of rock, but rarely consider temperature and damage into the model.

In order to ensure that the gas storage will not be damaged during construction and operation, it is necessary to analyze the stability of the gas storage. A large number of scholars (Istvan *et al*. 1997, Mortazavi and Nasab 2016) have studied the stability of gas storage, mainly based on the gas storage and rock mass mechanical properties in actual engineering, using numerical simulation to analyze the stability of gas storage. In order to more accurately simulate the actual engineering situation, a new creep constitutive model is often proposed for numerical simulation (Hosseini *et al*. 2012, Madurapperuma and Puswewala 2008). Therefore, it is necessary to program the new creep constitutive model, and the method of compiling, reading and applying through the secondary development interface of the numerical analysis software is simple and

*Corresponding author, Professor, Ph.D.
E-mail: baoyun666@cqust.edu.cn

ISSN: 2005-307X (Print), 2092-6219 (Online)

Fig. 1 Rock salt specimens

widely used. However, the creep model chosen for the calculation rarely considers the effects of temperature, which will bring some errors to the results. Therefore, it is necessary to establish a creep model that can more accurately describe the creep properties of rock salt.

This paper aims to build a nonlinear creep damage model that considers temperature damage and can describe the creep properties of rock salt. Based on the finite difference theory, the dynamic link calculation program (.dll) of the model is obtained by using VC++ program. The correctness of the nonlinear creep damage model and the calculation program is verified by laboratory test simulation calculation. The research results can provide reference for creep calculation of rock salt gas storage.

2. Temperature creep test of rock salt

2.1 Specimen preparation

Rock salt specimens were obtained during the drilling of oil and gas wells in western China, with a core depth of approximately 800-1000 m. The specimen had an average natural density of 2.17 g/cm^3. The core was machined into a cylindrical solid standard specimen of 100 mm in height and 50 mm in diameter (2:1 in height to diameter ratio) by dry sawing, as shown in Fig. 1. The size requirements of rock salt specimens are strictly in accordance with the International Rock Mechanics Society (ISRM) test procedure, in which the allowable error range is ±0.3mm, and the non-parallelism of the upper and lower end faces is ±0.05 mm. The wave velocity of the standard rock specimen is measured, and the rock specimens with similar wave velocity are selected for testing. The wave velocity of the rock salt specimen is about 3.030 km/s.

2.2 Creep tests

The triaxial creep test of rock salt at different temperatures adopts a grading loading method with constant confining pressure and constant temperature. The loading time of each stage is controlled at about 50h to ensure that the creep enters a stable stage, and it is loaded step by step until the rock salt specimen is destroyed. The confining pressure (σ_3) was constant at 3 MPa during the test, and the axial stress grading loading was carried out under the test conditions of 20°C (room temperature), 40°C, 60°C and 80°C, respectively. The axial stress of the creep test is determined by the peak stress (σ_c) at the corresponding temperature, and the low-to-high stepwise loading is taken as 20%σ_c, 40%σ_c, 60%σ_c, 80%σ_c, and 100%σc, respectively. The specific creep test conditions are shown in Table 1.

Table 1 Creep test conditions at different temperatures

No.	σ_3 /MPa	σ_c /MPa	T /℃	Axial stress/MPa				
				1st	2nd	3rd	4th	5th
A3	3	77.06	20	15.41	30.82	46.24	61.65	77.06
D1		67.24	40	13.45	26.90	40.34	53.79	67.24
B3		60.45	60	12.09	24.18	36.27	48.36	60.45
B9		52.83	80	10.57	21.13	31.70	42.26	52.83

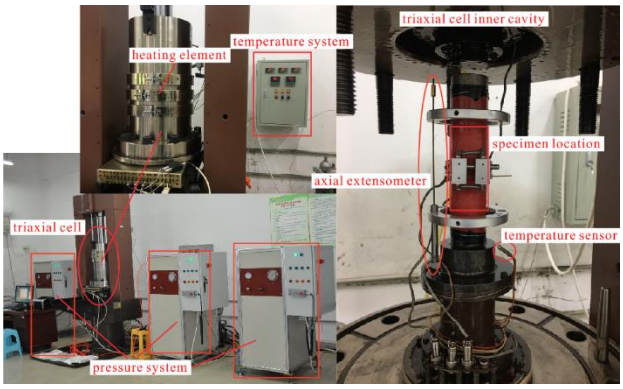

Fig. 2 TFD-2000 microcomputer servo-controlled rock triaxial rheometer

2.3 Test equipment

All creep tests were performed on TFD-2000 microcomputer servo-controlled rock triaxial rheometer (Fig. 2). The device is mainly composed of a shaft pressure system, a confining pressure system, a high-low temperature system and a pore water pressure system. The maximum axial force of the rheometer is 2000kN, and the maximum confining pressure is 100MPa. The temperature could be controlled from room temperature to 200°C. In the test, the data is automatically collected by the microcomputer and analyzed in real time. The specimen is placed between the two cushion blocks, and the axial extensometer is fixed on the upper and lower cushion blocks respectively. During the test, the heating elements is

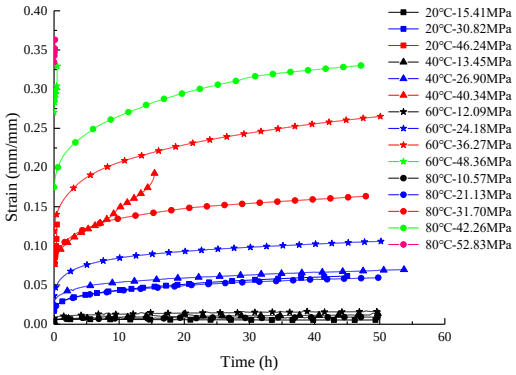

Fig. 3 Rock salt creep curves at different temperatures

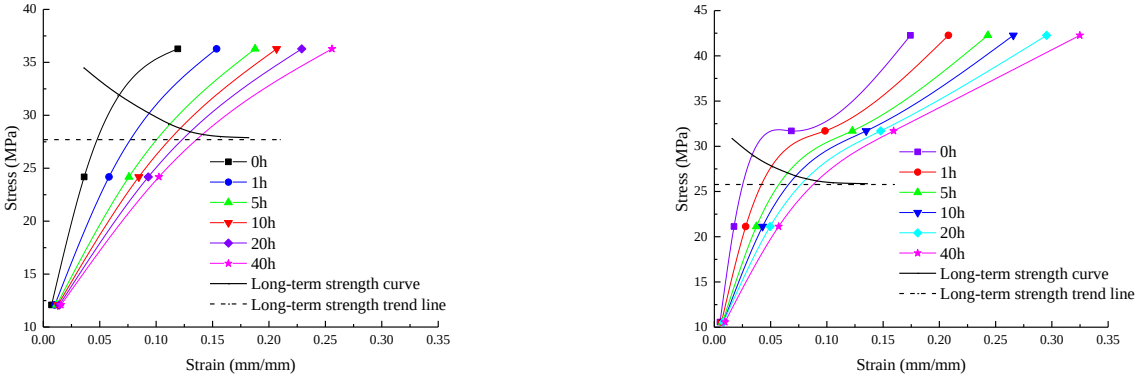

(a) T=60°C (b) T=80°C

Fig. 4 Isochronous stress-strain curve of rock salt

used to heat, and the temperature sensor inside the triaxial cell transmits the real-time temperature back to the temperature control system for automatic adjustment. Through real-time monitoring of temperature, it can be judged whether the temperature in the triaxial cell is stable. In addition, in order to ensure that the temperature inside the specimen is consistent, the temperature needs to be stable for 2 hours before applying axial pressure and confining pressure.

3. Creep characteristics and temperature effect of rock salt

3.1 Creep curve

The creep curve obtained by the grading loading is converted into a separately loaded creep curve cluster by processing, as shown in Fig. 3. It can be found that the rock salt creep curve mainly shows three typical creep stages: initial creep, steady creep and accelerated creep (Lv *et al*. 2019; Ladanyi 2006). In the case of low stress levels, rock salt generally only undergoes initial creep and steady state creep. When the stress level is high, three stages occur simultaneously in the rock salt creep process, such as the third stage at a temperature of 40°C. When the stress level reaches a certain height, it is possible that the initial creep and steady creep phases are short or the creep directly enters the accelerated creep phase, such as the last stages of temperatures of 20°C, 60°C, and 80°C.

3.2 Effect of temperature on long-term strength

It is generally considered that the critical stress value when the rock changes from steady creep to unsteady creep during the creep deformation process is called long-term strength (Cheon and Jung 2017; Nara *et al*. 2013). Only when the stress level is higher than the critical value, the rock will undergo creep damage. The methods for determining the long-term strength of rock are mainly the transition creep method and the isochronous curve method, and the most common one is the isochronous stress-strain curve method. The isochronous stress-strain curve refers to the relationship between the creep strain and stress corresponding to the same time in a set of creep curves at different stress levels. The isochronous stress-strain curve refers to the relationship between the creep strain and stress corresponding to the same time in a set of creep curves at different stress levels (Zhao and Koves 2012). Find the turning point where the straight line changes to the curve in all the curves, and the long-term strength is the stress value corresponding to the straight line formed by these points. According to this method, the isochronous stress-strain curves of the creep test under different temperature conditions are obtained, as shown in Fig. 4. It can be found that when the temperature is 60°C and 80°C, the long-term strength of the rock salt is 27.70 MPa and 25.78 MPa, respectively. Therefore, the long-term creep strength of rock

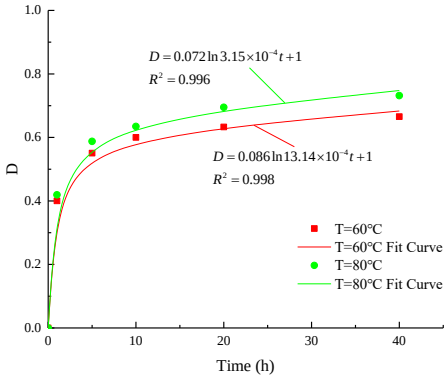

Fig. 5 Relationship between damage factor and creep time

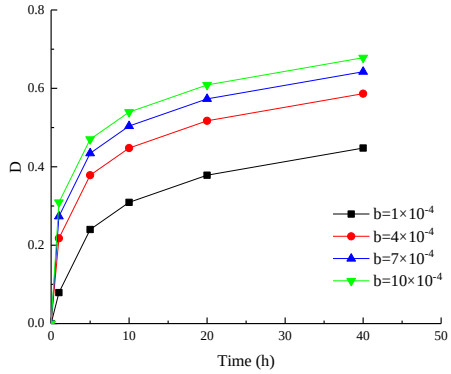

Fig. 6 Effect of parameters *b* on damage factors

salt decreases with increasing temperature.

3.3 Creep thermal damage evolution equation

There are two ways to define the rock damage, which is at the macroscale and the microscale, such as elastic modulus, stress, wave velocity, and the number of voids in the rock (Schubnel *et al*. 2006, Zahoor and Puri 2018). The most widely used method is the effective elastic modulus method, whose expression is:

$$D=\frac{E_0-E}{E_0} \tag{1}$$

wherein: E_0 is the elastic modulus of the initial lossless state and E is the effective elastic modulus.

From the isochronous stress-strain curve of Fig. 4, it can be seen that the slope of the curve decreases with increasing creep time, which is similar to the stress-strain curve of the triaxial test. Therefore, the creep modulus is defined by the method that the elastic modulus is the slope of the straight line segment of the stress-strain curve, that is, the creep modulus is the slope of the straight line segment of the stress-strain curve at different creep times in Fig. 4. The creep modulus at different times was calculated, and the damage modulus was calculated by replacing the effective elastic modulus with the creep modulus, and the relationship between the damage factor and the creep time was found (Fig. 5). It can be found that the relationship between the damage factor and the creep time is approximately logarithmic, and the early damage rate is faster and gradually decreases with time. The higher the temperature, the greater the creep damage of the rock salt, which is consistent with the conclusion that the long-term strength of the rock salt decreases with increasing temperature. The evolution equation of creep thermal damage of rock salt is obtained by fitting:

$$D=a\ln bt+1 \tag{2}$$

wherein: D is the damage factor, a and b are material parameters related to temperature, and t is time.

In order to determine the meaning of the parameter a, the two sides of the Eq. (2) are simultaneously derived:

$$\dot{D}=\frac{a}{t} \tag{3}$$

It can be seen from the above equation that the parameter a is proportional to the damage rate, and a can be defined as the damage rate factor of the whole process. The value of a is 0.072 and 0.086 at 60℃ and 80℃ respectively, indicating that the rock salt damage rate increases with increasing temperature.

At the same time, in order to determine the meaning of the parameter b, let a=0.1 and the parameter b take the values 1×10^{-4}, 4×10^{-4}, 7×10^{-4} and 10×10^{-4} respectively, and the influence of the parameter b is shown in Fig. 6. It can be seen from Fig. 6 that as the value of b increases, the damage value formed at the initial stage of creep becomes larger. Therefore, the parameter b controls the size of the damage variable in the early stage of creep, which can be defined as the damage speed factor in the early stage of creep. When the temperature is 60°C and 80°C, b is 3.15×10^{-4} and 13.1×10^{-4} respectively, indicating that the increase in temperature will cause the rock salt to reach a higher damage value in the early stage of creep.

4. Nonlinear thermal visco-elastic-plastic creep damage model of rock salt

4.1 Method for establishing nonlinear creep model

From Fig. 4, it can be found that the relationship between stress and strain at the same time is nonlinear. In the figure, the isochronous stress-strain relationship is a curve, which reflects the nonlinear creep characteristics of the rock creep process. There are four methods for solving nonlinear creep problems commonly used at present (Zuo *et al*. 2018):

(1) For the case where the nonlinear creep characteristics are not obvious, a linear creep model (such as Nishihara model, Burgers model, etc.) is combined with a nonlinear viscous element. The nonlinear viscous element is connected in series to the visco-plastic part of the linear creep model to achieve the effect of correcting the linear creep model.

(2) The corresponding empirical constitutive relation is obtained by fitting the test results of the laboratory creep test.

(3) By modifying the linear creep model and processing the parameters of linear elements (such as E, η) in the linear

Table 2 Inversion parameters of Burgers creep model

T (℃)	σ_1 (MPa)	K_1 (MPa)	G_1 (MPa)	η_1 (MPa·h)	G_2 (MPa)	η_2 (MPa·h)	R^2
20	30.82	959.06	345.61	18941.18	478.33	1871.51	0.993
40	13.45	1047.21	1071.30	63399.97	859.34	3812.786	0.855
40	26.90	392.93	397.89	23083.19	352.61	1154.51	0.994
60	12.09	372.00	5407.16	43476.69	672.41	2688.94	0.952
60	24.18	230.12	277.81	14653.56	175.66	576.60	0.995
60	36.27	94.49	292.28	8531.39	151.43	649.21	0.996
80	10.57	784.31	395.27	64698.80	1397.32	2576.95	0.851
80	21.13	303.00	2197.36	16352.96	290.98	1296.76	0.994
80	31.70	6255.19	47.28	15471.33	184.65	759.37	0.995
80	42.26	145.18	62.85	11072.38	162.91	1043.47	0.994

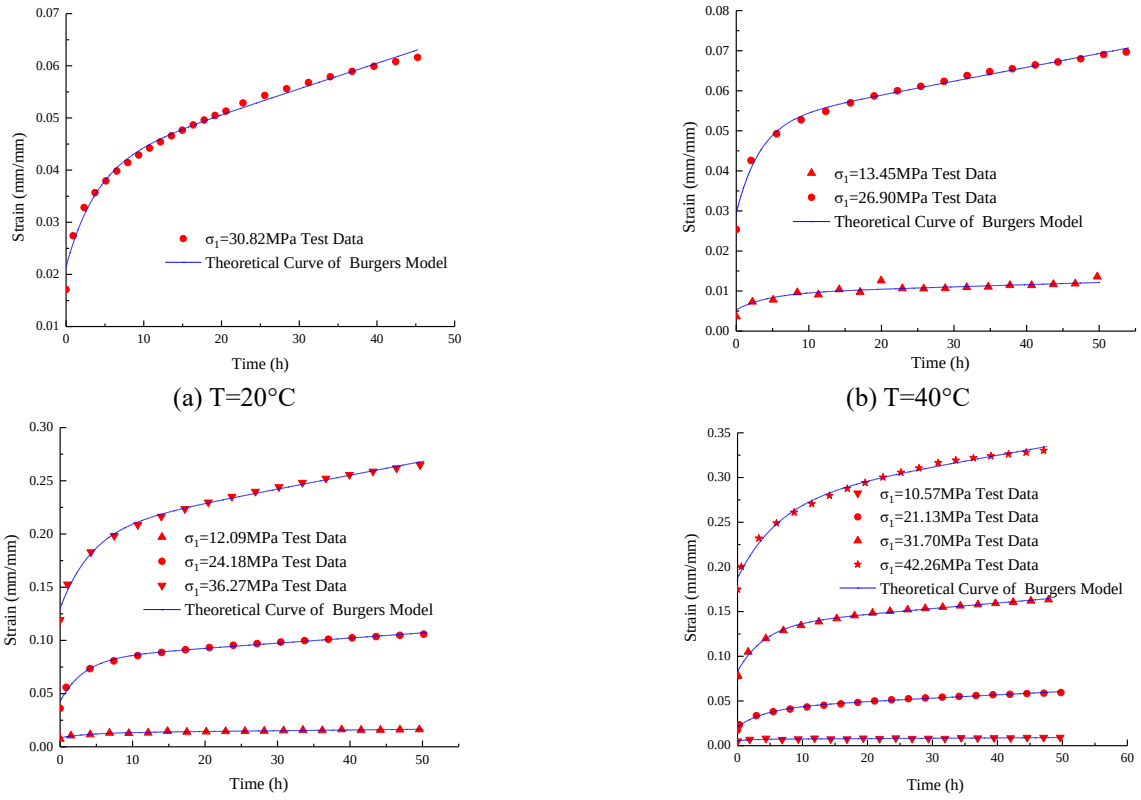

(a) T=20°C (b) T=40°C

(c) T=60°C (d) T=80°C

Fig. 7 Burgers theoretical curve versus test data

creep model, the linear elements are converted into nonlinear elements, where the parameters are determined by the test, and then derive a nonlinear creep constitutive relations. This method is more rigorous in academic theory and has an ideal effect.

(4) Apply new theories. Such as the newly developed theory of artificial intelligence, fracture mechanics and damage mechanics.

The nonlinear creep model established by the above method can better describe the three stages of rock creep. This paper combines the first and third methods to establish a nonlinear creep damage model of rock salt under different temperatures.

4.2 Fitting of burgers creep model

It can be seen from Fig. 3 that the creep curve of salt rock without accelerated creep has the following characteristics: in the initial creep stage, the salt rock will produce instantaneous elastic strain. In the steady creep stage, the creep strain continues to increase with the increase of time. At the same time, the creep rate gradually stabilized. Therefore, the salt rock creep model without accelerated creep should include elastic elements and viscous elements, that is, showing visco-elastic characteristics. Some scholars (Okuka and Zorica 2019; Eslami Andargoli *et al*. 2018) have shown that the Burgers creep model can well describe the creep characteristics of

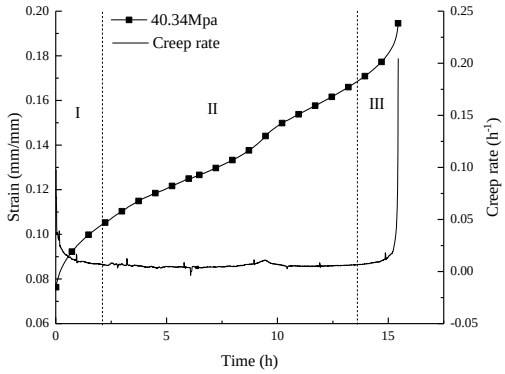

(a) T=40°C, σ_1=40.34 MPa

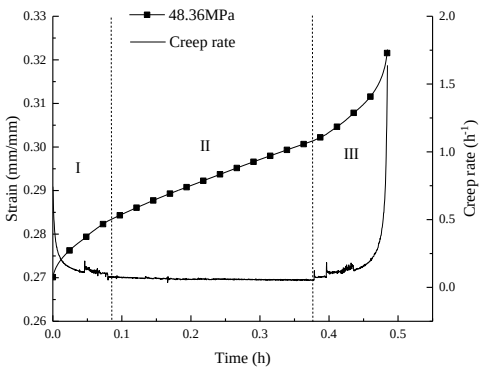

(b) T=60°C, σ_1=48.36 MPa

Fig. 8 Accelerated creep curve and creep rate

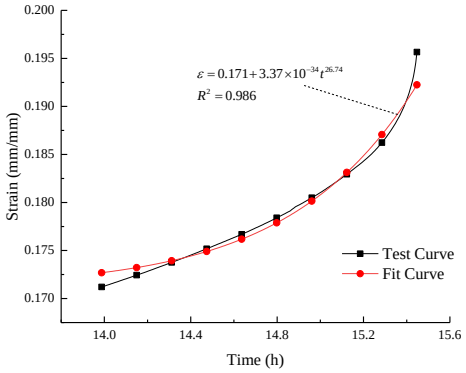

(a) T=40°C , σ_1=40.34 MPa

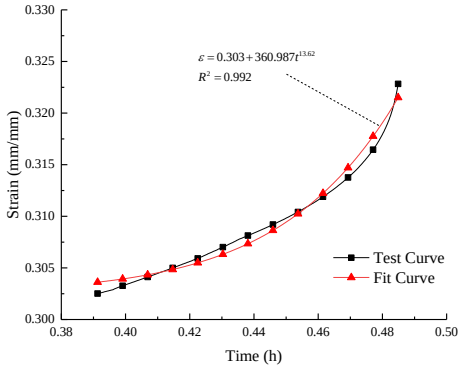

(b) T=60°C , σ_1=48.36 MPa

Fig. 9 Accelerated creep curve versus fitted curve

rock under stress levels without accelerated creep. Therefore, a nonlinear creep model of salt rock can be established based on the Burgers creep model. The tri-axial creep equation of Burgers model is (Zhang *et al*. 2012):

$$\frac{\sigma_1-\sigma_3}{3G_1}+\frac{\sigma_1+2\sigma_3}{9K_1}+\frac{\sigma_1-\sigma_3}{3\eta_1}t+\frac{\sigma_1-\sigma_3}{3G_2}\left(1-\exp\left(-\frac{G_2}{\eta_2}t\right)\right) \quad (4)$$

Based on the salt rock creep test data, the parameters of the Burgers creep model are inverted. The results of the parameter inversion are shown in Table 2. In order to verify and show the rationality of the fitted parameters, the theoretical results of the Burgers creep model and the results of the creep test are compared, as shown in Fig. 7. It can be seen from Fig. 7 that the Burgers theoretical curve is consistent with the test data, indicating that the Burgers creep model can better describe the initial and steady creep stages of rock salt.

4.3 Nonlinear thermal visco-plastic damage model

Fig. 8 is the curve of the accelerated creep stage of rock salt during creep process, in which III is the accelerated creep stage. It can be seen that the creep strain in the III stage shows obvious nonlinear characteristics with time. Therefore, it is necessary to establish a nonlinear creep model to describe the whole process of rock salt creep. At the same time, in order to reflect the creep characteristics of the salt rock when the temperature changes, the temperature damage is taken into account in the creep model.

It is found that the acceleration creep curve is similar to the power function curve, so the acceleration creep phase can be fitted by a power function:

$$\varepsilon=\varepsilon_0+At^n \quad (5)$$

wherein: ε is the creep strain, ε_0 is the initial strain value at which accelerated creep occurs, A is the fitting parameter (representing the stress duration state), t is the creep time, and n is the accelerated creep parameter.

Applying Eq. (4) to fit the accelerated creep curve (Fig. 9), it is found that the power function is consistent with the accelerated creep curve, and the correlation coefficient (R^2) is greater than 0.98, indicating that the power function can well describe the accelerated creep.

In order to describe nonlinear features with viscous elements, while taking into account the effects of temperature damage, the elements need to be processed unconventionally. First, the two sides of the Eq. (5) are simultaneously derived:

$$\dot{\varepsilon}=nAt^{n-1} \quad (6)$$

Since the stress σ is constant during creep, nA is a constant. Let $nA=\sigma/\eta_0$, where η_0 is a constant indicating the viscosity coefficient at the beginning of accelerated creep, then Eq. (6) can be transformed into the following formula:

$$\dot{\varepsilon} = \frac{\sigma}{\eta_0 / t^{n-1}} \tag{7}$$

The constitutive equation of the viscous element can be expressed as $\dot{\varepsilon} = \sigma/\eta$, and considering the effects of temperature damage D, there are:

$$\eta(D) = \eta(1-D) \tag{8}$$

The damage factor is a logarithmic function with time, and the viscosity coefficient η in the viscous element is processed by combining Eq. (2), Eq. (7), and Eq. (8) to obtain:

$$\eta(n,t,D) = \frac{\eta_0}{a\ln(bt)\cdot t^{n-1}} = \frac{\eta_0}{a\ln(bt)}\frac{t_0^{n-1}}{t^{n-1}} \tag{9}$$

wherein: t_0 is the unit reference time.

Substituting Eq. (9) into the constitutive equation of the viscous element, the constitutive equation expression of the nonlinear thermal viscous element can be obtained as follows:

$$\dot{\varepsilon} = \frac{\sigma}{\eta(n,t,D)} = \frac{\sigma \cdot a\ln(bt)}{\eta_0}\frac{t^{n-1}}{t_0^{n-1}} = \frac{\sigma \cdot a\ln(bt)}{\eta_0}t^{n-1} \tag{10}$$

Based on the above method of establishing a nonlinear creep model, a new nonlinear thermal visco-plastic damage model can be obtained by paralleling the treated nonlinear thermal viscous element with the plastic element, as shown in Fig. 10. The model can better reflect the accelerated creep phase of rock salt, and its creep constitutive equation can be expressed as:

$$\varepsilon(t) = \frac{H(\sigma-\sigma_\infty)}{\eta_{(n,t,D)}}t = \frac{H(\sigma-\sigma_\infty)}{\eta_0}\frac{a\ln(bt)\cdot t^n}{t_0^{n-1}} = \frac{H(\sigma-\sigma_\infty)}{\eta_0}a\ln(bt)\cdot t^n \tag{11}$$

wherein: σ_∞ is the long-term strength, and the expression for H is:

$$H(\sigma-\sigma_\infty) = \begin{cases} 0 & \sigma \le \sigma_\infty \\ \sigma-\sigma_\infty & \sigma > \sigma_\infty \end{cases} \tag{12}$$

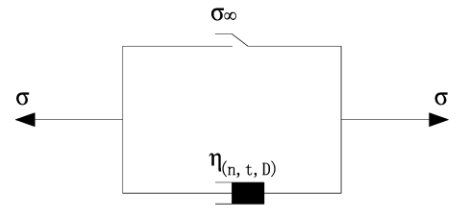

Fig. 10 Nonlinear thermal visco-plastic damage model

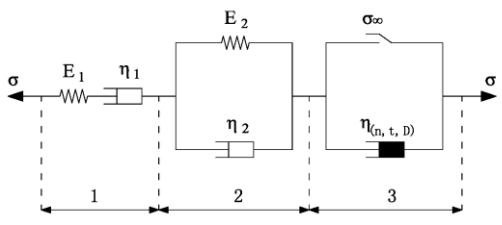

Fig. 11 Nonlinear thermal visco-elastic-plastic creep damage model

4.4 Nonlinear thermal visco-elastic-plastic damage model

A nonlinear thermal visco-elastic-plastic creep damage model (hereinafter referred to as a nonlinear T-VEPD creep model) with a six-element combination is constructed by the Burgers model in series with the nonlinear thermal visco-plastic damage model, as shown in Fig. 11. The model can better describe the accelerated creep properties of rock salt under temperature and stable stress. It should be noted that in the following formula derivation process, in order to simplify the expression in the formula, the stress and strain of parts 1, 2 and 3 in the model are represented by σ_1, σ_2, σ_3, ε_1, ε_2 and ε_3 respectively; The initial value of the viscosity coefficient $\eta_{(n,t,D)}$ is represented by η_3.

When $0<\sigma\le\sigma_\infty$, the friction plate in the third part is a rigid body, and the model is equivalent to the Burgers model composed of parts 1 and 2. The constitutive equation is:

$$\sigma + \left(\frac{\eta_1}{E_1} + \frac{\eta_1+\eta_2}{E_2}\right)\dot{\sigma} + \frac{\eta_1\eta_2}{E_1E_2}\ddot{\sigma} = \eta_1\dot{\varepsilon} + \frac{\eta_1\eta_2}{E_2}\ddot{\varepsilon} \tag{13}$$

When $\sigma>\sigma_\infty$, the thermal visco-plastic component participates in creep, and the equation of state can be expressed as:

$$\begin{cases} \sigma = \sigma_1 = \sigma_2 = \sigma_3 \\ \varepsilon = \varepsilon_1 + \varepsilon_2 + \varepsilon_3 \\ \dot{\varepsilon}_1 = \dot{\sigma}_1/E_1 + \sigma_1/\eta_1 \\ \sigma_2 = E_2\varepsilon_2 + \eta_2\dot{\varepsilon}_2 \\ \sigma_3 = \sigma_\infty + \eta_3\varepsilon_3 / \left[a\ln(bt)\cdot t^n\right] \end{cases} \tag{14}$$

Wherein: a is the total stress and b is the total strain.

The constitutive equation obtained according to Eq. (14) is expressed as:

$$\begin{aligned} E_2\dot{\varepsilon} + \eta_2\ddot{\varepsilon} = {} & \frac{E_2}{\eta_1}\sigma + \left(\frac{\eta_2}{\eta_1} + \frac{E_1+E_2}{E_1} + \frac{E_2}{\eta_3}t + \frac{\eta_2}{\eta_3}\cdot 2\left(n + \frac{1}{\ln(bt)}\right)\right)\dot{\sigma} \\ & + \left(\frac{\eta_2}{E_1} + \frac{\eta_2}{\eta_3}t\right)\ddot{\sigma} + \frac{\sigma-\sigma_\infty}{\eta_3}\left(E_2\left(n + \frac{1}{\ln(bt)}\right) + \left(\frac{n(n-1)}{t} - \frac{1}{\ln(bt)}\right)\right) \end{aligned} \tag{15}$$

When $0<\sigma\le\sigma_\infty$ and $\sigma>\sigma_\infty$, keep $\sigma=\sigma_0$ and constant, and perform Laplace transform and inverse transform on Eq. (13) and Eq. (15) respectively, and obtain the creep equation of the nonlinear T-VEPD creep model:

$$\begin{cases} \varepsilon = \dfrac{\sigma_0}{E_1} + \dfrac{\sigma_0}{\eta_1}t + \dfrac{\sigma_0}{E_2}\left(1 - \exp\left(-\dfrac{E_2}{\eta_2}t\right)\right) & \sigma \le \sigma_\infty \\ \varepsilon = \dfrac{\sigma_0}{E_1} + \dfrac{\sigma_0}{\eta_1}t + \dfrac{\sigma_0}{E_2}\left(1 - \exp\left(-\dfrac{E_2}{\eta_2}t\right)\right) + \dfrac{\sigma_0-\sigma_\infty}{\eta_3}a\ln(bt)t^n & \sigma > \sigma_\infty \end{cases} \tag{16}$$

In order to accurately calculate the stress and strain states under the three-dimensional force state, the three-dimensional creep equation is derived from Eq. (16). Under three-dimensional stress conditions, the total strain of the nonlinear T-VEPD creep model is the sum of three parts:

$$\varepsilon = \varepsilon_{1ij} + \varepsilon_{2ij} + \varepsilon_{3ij} \tag{17}$$

Table 3 Inversion parameters of nonlinear T-VEPD creep model

T (℃)	σ_1 (MPa)	K_1 (MPa)	G_1 (MPa)	η_1 (MPa·h)	G_2 (MPa)	η_2 (MPa·h)	η_3 (MPa·h)	a	b	n	R^2
20	46.24	957.21	189.66	412.25	737.36	402.35	522.75	69.632	2.804	2.31	0.995
40	40.34	2618.3	166.69	511.80	1651.67	1191.64	851.59	0.357	0.005	1.34	0.997
60	36.27	1136.8	101.03	570.26	1371.74	429.77	118.859	0.052	0.001	1.49	0.983
60	48.36	1086.85	55.90	321.91	1046.97	399.46	91.01	75.63	2.703	6.78	0.997
80	31.70	965.75	179.01	566.53	1634.37	365.62	84.16	0.061	0.002	1.56	0.963
80	42.62	632.31	237.48	501.24	1059.61	418.60	623.15	0.063	0.004	2.04	0.974

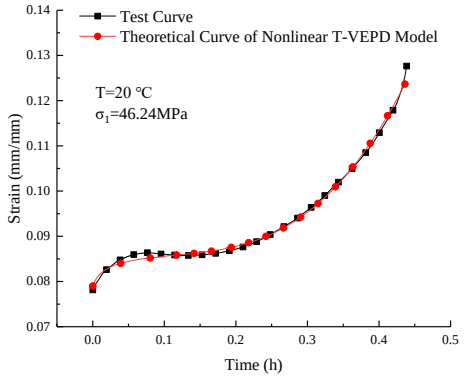

(a) T=20°C, σ_1=46.24MPa

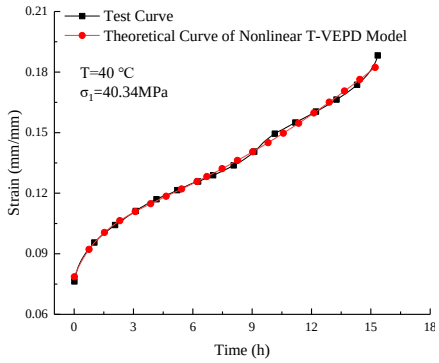

(b) T=40°C, σ_1=40.34 MPa

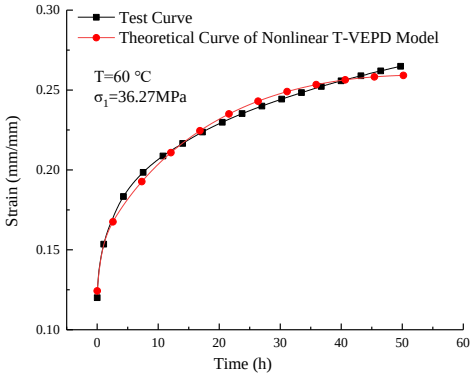

(c) T=60°C, σ_1=36.27 MPa

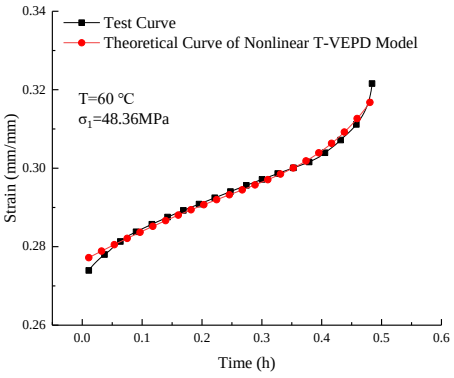

(d) T=60°C, σ_1=48.36 MPa

Fig. 12 Creep test curve versus theoretical curve

According to hook law, the three-dimensional constitutive model of an elastic body is:

$$\sigma_{kk} = 3K\varepsilon_{kk} \qquad e_{ij} = \frac{S_{ij}}{2G} \tag{18}$$

Wherein: σ_{kk} is the stress tensor, ε_{kk} is the first invariant of strain tensor, S_{ij} is the partial stress tensor, e_{ij} is the partial strain tensor, K is the bulk modulus, and G is the shear modulus.

Therefore, the three-dimensional constitutive equation of the elastic body and viscous body in Part 1 is:

$$\varepsilon_{1ij} = \frac{S_{ij}}{2G_1} + \frac{\sigma_m \delta_{ij}}{3K_1} + \frac{S_{ij}}{2\eta_1} t \tag{19}$$

Wherein: $\sigma_m \delta_{ij}$ is the spherical stress tensor.

Assuming that the volume change is elastic, the rheological properties are mainly reflected in the shear deformation. The three-dimensional constitutive equation of the viscoelastic body in Part 2 is:

$$\varepsilon_{2ij} = \frac{S_{ij}}{2G_2}\left[1 - \exp\left(-\frac{G_2}{\eta_2} t\right)\right] \tag{20}$$

When $S_{ij} > \sigma_\infty$, the three-dimensional constitutive equation of Part 3 is:

$$\varepsilon_{3ij} = \frac{S_{ij} - \sigma_\infty}{2\eta_3} a \ln(bt) t^n \tag{21}$$

Under the condition of triaxial compression test, there is $\sigma_2 = \sigma_3$, so there is the following relationship:

$$\sigma_m = 3(\sigma_1 + 2\sigma_3) \qquad S_{11} = \sigma_1 - \sigma_m = \frac{2}{3}(\sigma_1 - \sigma_3) \tag{22}$$

Combining Eqs. (16)-(22), the axial creep equation of

the nonlinear T-VEPD creep model under the three-dimensional stress state is:

$$\varepsilon_1=\begin{cases}\dfrac{\sigma_1-\sigma_3}{3G_1}+\dfrac{\sigma_1+2\sigma_3}{9K_1}+\dfrac{\sigma_1-\sigma_3}{3\eta_1}t+\dfrac{\sigma_1-\sigma_3}{3G_2}\left(1-\exp\left(-\dfrac{G_2}{\eta_2}t\right)\right) & \sigma_1-\sigma_3\le\sigma_\infty \\ \dfrac{\sigma_1-\sigma_3}{3G_1}+\dfrac{\sigma_1+2\sigma_3}{9K_1}+\dfrac{\sigma_1-\sigma_3}{3\eta_1}t+\dfrac{\sigma_1-\sigma_3}{3G_2}\left(1-\exp\left(-\dfrac{G_2}{\eta_2}t\right)\right)+\dfrac{\sigma_1-\sigma_3-\sigma_\infty}{3\eta_3}a\ln(bt)t^n & \sigma_1-\sigma_3>\sigma_\infty\end{cases} \tag{23}$$

4.5 Model parameters inversion and verification

According to the obtained rock salt nonlinear T-VEPD creep model, when $0<\sigma_1-\sigma_3\le\sigma_\infty$, the nonlinear T-VEPD creep model is equivalent to Burgers creep model. Therefore, the rock salt creep test data of various conditions in which the stress level satisfies $\sigma_1-\sigma_3>\sigma_\infty$ is subjected to parameter inversion, and the creep parameters are as shown in Table 3. Fig. 12 is a comparison of the nonlinear T-VEPD creep model with the experimental data.

From Table 3, the following findings are found: (1) The fitting parameter correlation coefficient (R^2) is above 0.96, indicating that the model can well describe the rock salt creep curve characteristics. (2) The values of parameters *a* and *b* under conditions of accelerated creep are much larger than those without acceleration creep. This is because the parameters a and b are positively correlated with the rock salt damage, that is, the damage degree and the damage speed of the rock salt in the accelerated creep stage increase rapidly, resulting in an increase in the parameters *a* and *b*. (3) When the temperature remains unchanged, as the stress level increases, the shear modulus *G* and the bulk modulus *K* decreases.

It can be seen from Fig. 12 that the theoretical curve is in good agreement with the experimental curve. The model not only can describe the initial stage and the steady state stage of creep well, but also better describe the accelerated creep stage. That is, the model can better describe the whole process of rock salt creep, indicating the rationality of the proposed nonlinear T-VEPD creep model.

5. Implementation of nonlinear T-VEPD creep model in FLAC^{3D}

5.1 Finite difference of nonlinear T-VEPD creep model

In order to apply the nonlinear creep model to numerical simulation, the finite difference form of the model is required. Then programmatically generate a calculation program (.dll) that can be read directly by FLAC^{3D}. Move the generated calculation program to the position that FLAC^{3D} can call, so that it can be read and calculated by FLAC^{3D}.

The nonlinear T-VEPD creep model consists of 3 parts connected in series (Fig. 11), so the stress is equal and the strain is added:

$$\begin{aligned}&S_{ij}=S_{1ij}=S_{2ij}=S_{3ij}\\&e_{ij}=e_{1ij}+e_{2ij}+e_{3ij}\end{aligned} \tag{24}$$

The part 1 is the Maxwell body. The relationship between partial stress and partial strain rate is as follows:

$$\dot{e}_{1ij}=\frac{\dot{S}_{ij}}{2G_1}+\frac{S_{ij}}{2\eta_1} \tag{25}$$

The part 2 is the Kelvin body. The relationship between deviating stress and deviating strain is as follows:

$$S_{ij}=2\eta_2\dot{e}_{2ij}+2G_2e_{2ij} \tag{26}$$

For part 3 there are:

$$\dot{e}_{3ij}=\frac{\{\phi(F)\}}{2\eta_3} \tag{27}$$

wherein: $\eta_3=\eta_{(n,t,T,D)}=\eta_0/\left(a\ln(bt)t^n\right)$, η_0 is the viscosity coefficient of the initial acceleration period, $F=\sigma_1-\sigma_3-\sigma_\infty$ is the yield function, $\phi(F)=\begin{cases}0 & F<0\\ F & F\ge0\end{cases}$ is the switching function.

Convert the strain in Eq. (24) to incremental form:

$$\Delta e_{ij}=\Delta e_{1ij}+\Delta e_{2ij}+\Delta e_{3ij} \tag{28}$$

After calculating and sorting Eqs. (25)-(27) using the central difference, the incremental form of each part is obtained:

$$\Delta e_{1ij}=e_{1ij}^N-e_{1ij}^O=\frac{\Delta S_{ij}}{2G_1}+\frac{\bar{S}_{ij}}{2\eta_1}\Delta t \tag{29}$$

$$\Delta e_{2ij}=e_{2ij}^N-e_{2ij}^O=\frac{1}{A}\left[\left(S_{ij}^N+S_{ij}^O\right)\frac{\Delta t}{4\eta_2}-(A+B)e_{2ij}^O\right] \tag{30}$$

$$\Delta e_{3ij}=e_{3ij}^N-e_{3ij}^O=\frac{\bar{S}_{ij}-\frac{2}{3}\sigma_\infty}{2\eta_3}\Delta t\quad F\ge0 \tag{31}$$

wherein: $\bar{S}_{ij}=\dfrac{\left(S_{ij}^N+S_{ij}^O\right)}{2}$ is the average partial stress, where $\bar{e}_{ij}=\dfrac{\left(e_{ij}^N+e_{ij}^O\right)}{2}$ is the average partial strain, the superscripts ^{N} and ^{o} in the formula represent the new and old states, respectively, $A=1+\dfrac{G_2\Delta t}{2\eta_2}$, $B=\dfrac{G_2\Delta t}{2\eta_2}-1$.

Substituting Eqs. (29)-(31) into Eq. (28) and sorting out the stress update formula of the nonlinear T-VEPD creep model:

$$\begin{cases}S_{ij}^N=\dfrac{1}{X_1}\left[\Delta e_{ij}+\left(\dfrac{B}{A}+1\right)e_{2ij}^O+Y_1S_{ij}^O\right] & F<0\\ S_{ij}^N=\dfrac{1}{X_2}\left[\Delta e_{ij}+\left(\dfrac{B}{A}+1\right)e_{2ij}^O+Y_2S_{ij}^O+\dfrac{\sigma_\infty}{3\eta_3}\Delta t\right] & F\ge0\end{cases} \tag{32}$$

Wherein: $X_1 = \frac{1}{2G_1} + \frac{\Delta t}{4\eta_1} + \frac{\Delta t}{4A\eta_2}$, $Y_1 = \frac{1}{2G_1} - \frac{\Delta t}{4\eta_1} - \frac{\Delta t}{4A\eta_2}$, $X_2 = \frac{1}{2G_1} + \frac{\Delta t}{4\eta_1} + \frac{\Delta t}{4A\eta_2} + \frac{\Delta t}{4\eta_3}$, $Y_2 = \frac{1}{2G_1} - \frac{\Delta t}{4\eta_1} - \frac{\Delta t}{4A\eta_2} - \frac{\Delta t}{4\eta_3}$.

5.2 Validation of nonlinear T-VEPD creep model program

In order to verify the correctness of the nonlinear thermal visco-elastic-plastic creep damage model calculation program (.dll), the numerical simulation was carried out by the rock salt triaxial creep test. The model is a cylindrical specimen with a height of 100 mm and a diameter of 50 mm. The normal deformation is carried out at the bottom of the model, the normal load is applied to the top, and the surface load is applied to the circumferential normal to simulate the confining pressure. Due to the obvious accelerated creep stage of the D1 specimen, the loading scheme was loaded with a confining pressure of 3 MPa, a temperature of 40℃, and a three-stage axial pressure (13.45 MPa, 26.90 MPa, and 40.34 MPa). The creep model adopts the compiled model, the creep parameters adopt the parameters under the corresponding conditions in Table 2 and Table 3. The basic mechanical parameters adopt relevant test results (Zhao *et al*. 2019), as shown in Table 4.

Through the simulation calculation, the vertical displacement curve of the center point of the upper end surface of the cylinder and the Y-direction (vertical) displacement cloud map are obtained (Fig. 13). It can be seen that when the axial stress is 13.45 MPa and 26.90 MPa, the simulation curve shows two stages of initial creep and steady creep. When the axial stress is 40.34 MPa, the model curve shows the whole process of initial creep, steady creep and accelerated creep, which is consistent with the trend of the test curve under the same conditions. In the simulation calculation, the creep calculation time of the first two stages is 50h, and the third level is 22.5h. When the stress is 13.45 MPa and 26.90 MPa, the calculated maximum displacements are 1.52 mm and 7.57mm, respectively, and the maximum deformation of the specimens in the test are 1.42mm and 6.98 mm, respectively. When the stress is 40.34 MPa, the acceleration creep stage is entered at 20 h during the calculation, and the accelerated creep is entered at 14.85 h in the test, and the deformations when the two enter the accelerated creep are 19.6 mm and 17.9 mm, respectively. In summary, the simulation curve is consistent with the actual test curve regardless of the trend of change and the magnitude of creep deformation, indicating the rationality and correctness of the nonlinear creep model.

6. Conclusions

Based on the triaxial creep test of rock salt under different temperatures, the nonlinear creep damage model of rock salt is established, and the validity of the model is verified. In summary,

• Temperature can degrade the long-term strength of rock salt. The creep modulus is defined by the slope of the isochronous stress-strain curve. Then the damage modulus is obtained by the equivalent elastic modulus method. The relationship between the damage factor and the creep time at different temperatures is found. The results show that the higher the temperature, the greater the damage during the creep process of rock salt; the relationship between damage factor and creep time is approximately logarithmic, and the damage rate is faster in the early stage and gradually decreases with time.

• According to the nonlinear characteristics appearing in the creep test, the nonlinear thermal visco-plastic damage model of rock salt under temperature is proposed. By using the nonlinear creep model construction method, the obtained thermal visco-plastic damage model is connected with the Burgers creep model to obtain a nonlinear thermal visco-elastic-plastic creep damage model which can better reflect the accelerated creep behavior of rock salt. The obtained model is compared with the experimental data, and the fitting degree is high, which indicates that the model can well describe the creep characteristics of rock salt.

• Using the finite difference theory, the finite difference expression form of the rock salt nonlinear T-VEPD creep model is derived. The dynamic link calculation program of the model is obtained by programming combined with the secondary development interface of FLAC^{3D}. The correctness of the model calculation program is verified by experimental simulation.

Acknowledgments

The authors gratefully acknowledge financial support from the Chongqing Research Program of Basic Research and Frontier Technology (cstc2016jcyjA0302), Scientific and Technological Research Program of Chongqing Municipal Education Commission (KJ1713324), Sponsored by Research Fund for Excellent Dissertation of China Three Gorges University (2021BSPY015).

References

Cheon, D.S. and Jung, Y.B. (2017), "Analysis of acoustic emission signals during long-term strength tests of brittle materials", *Tunn. Undergr. Sp. Technol*., **27**(3), 121-131. https://doi.org/10.7474/TUS.2017.27.3.121.

Eslami Andargoli, M. B., Shahriar, K., Ramezanzadeh, A. and Goshtasbi, K. (2018), "The analysis of dates obtained from long-term creep tests to determine creep coefficients of rock salt", *B. Eng. Geol. Environ*., **78**(3), 1617-1629. https://doi.org/10.1007/s10064-018-1243-4.

Fahimifar, A., Tehrani, F.M., Hedayat, A. and Vakilzadeh, A. (2010), "Analytical solution for the excavation of circular tunnels in a visco-elastic burger's material under hydrostatic stress field", *Tunn. Undergr. Sp. Technol*., **25**(4), 297-304. https://doi.org/10.1016/j.tust.2010.01.002.

Haupt, M. (1991), "A constitutive law for rock salt based on creep and relaxation tests", *Rock Mech. Rock Eng*., **24**(4), 179-206. https://doi.org/10.1007/BF01045031.

Hosseini, E., Holdsworth, S.R. and Mazza, E. (2012), "Creep

constitutive model considerations for high-temperature finite element numerical simulations", *J. Strain Anal. Eng. Des.*, **47**(6), 341-349. https://doi.org/10.1177/0309324712450542.

Istvan, J.A., Evans, L.J., Weber, J.H. and Devine, C. (1997), "Rock mechanics for gas storage in bedded salt caverns", *Int. J. Rock Mech. Min. Sci.*, **34**(3-4), 647-647. https://doi.org/10.1016/s1365-1609(97)00108-1.

Gray, V. and Whittaker, M. (2015), "Development and assessment of a new empirical model for predicting full creep curves", *Materials*, **8**(7), 4582-4592. https://doi.org/10.3390/ma8074582.

Khaledi, K., Mahmoudi, E., Datcheva, M. and Schanz, T. (2016), "Analysis of compressed air storage caverns in rock salt considering thermo-mechanical cyclic loading", *Environ. Earth Sci.*, **75**(15), 1-17. https://doi.org/10.1007/s12665-016-5970-1.

Ladanyi, B. (2006), "Creep of frozen slopes and ice-filled rock joints under temperature variation", *Can. J. Civ. Eng.*, **33**(6), 719-725. https://doi.org/10.1139/l05-112.

Leoni, M., Karstunen, M. and Vermeer, P. A. (2008), "Anisotropic creep model for soft soils", *Géotechnique*, **58**(3), 215-226. https://doi.org/10.1680/geot.2008.58.3.215.

Lv, S., Wang, W. and Liu, H. (2019), "A creep damage constitutive model for a rock mass with nonpersistent joints under uniaxial compression", *Math. Prob. Eng.*, 1-11. https://doi.org/10.1155/2019/4361458.

Lyakhovsky, V., Hamiel, Y. and Ben-Zion, Y. (2011), "A non-local visco-elastic damage model and dynamic fracturing", *J. Mech. Phys. Solids*, **59**(9), 1752-1776. https://doi.org/10.1016/j.jmps.2011.05.016.

Madurapperuma, M.A.K. and Puswewala, U.G. (2008), "Numerical implementation of a constitutive model for soil creep", *J. Mech. Mater. Struct.*, **3**(10), 1857-1874. https://doi.org/10.2140/jomms.2008.3.1857.

Mortazavi, A. and Nasab, H. (2016), "Analysis of the behavior of large underground oil storage caverns in salt rock", *In. J. Numer. Anal. Meth. Geomech.*, **41**(4), 602-624. https://doi.org/10.1002/nag.2576.

Nara, Y., Yamanaka, H., Oe, Y. and Kaneko, K. (2013), "Influence of temperature and water on subcritical crack growth parameters and long-term strength for igneous rocks", *Geophys. J. Int.*, **193**(1), 47-60. https://doi.org/10.1093/gji/ggs116.

Nazary Moghadam, S., Nazokkar, K., Chalaturnyk, R.J. and Mirzabozorg, H. (2015), "Parametric assessment of salt cavern performance using a creep model describing dilatancy and failure", *Int. J. Rock Mech. Min. Sci.*, **79**, 250-267. https://doi.org/10.1016/j.ijrmms.2015.06.012.

Obst, K. (2019), "From salt mining and hydrocarbon exploration towards geothermal use and natural gas storage in the eastern part of the North German Basin", *Zeitschrift der Deutschen Gesellschaft fur Geowissenschaften*, **170**(3-4), 357-380. https://doi.org/10.1127/zdgg/2019/0207.

Okuka, A.S. and Zorica, D. (2019), "Fractional Burgers models in creep and stress relaxation tests", *Appl. Math. Modell.*, **77**, 1894-1935. https://doi.org/10.1016/j.apm.2019.09.035.

Pestrenin, V.M. and Pestrenina, I.V. (2010), "Nonlinear hereditary model of the prestressed salt rocks", *J. Min. Sci.*, **46**(1), 21-27. https://doi.org/10.1007/s10913-010-0003-z.

Schubnel, A., Benson, P.M., Thompson, B.D., Hazzard, J.F. and Young, R.P. (2006), "Quantifying Damage, Saturation and Anisotropy in Cracked Rocks by Inverting Elastic Wave Velocities", *Pure Appl. Geophys.*, **163**(5-6), 947-973. https://doi.org/10.1007/s00024-006-0061-y.

Sharifzadeh, M., Tarifard, A. and Moridi, M.A. (2013), "Time-dependent behavior of tunnel lining in weak rock mass based on displacement back analysis method", *Tunn. Undergr. Sp. Technol.*, **38**, 348-356. https://doi.org/10.1016/j.tust.2013.07.014.

Shkuratnik, V.L., Kravchenko, O.S. and Filimonov, Y.L. (2019), "Stresses and temperature affecting acoustic emission and rheological characteristics of rock salt", *J. Min. Sci.*, **55**(4), 531-537. https://doi.org/10.1134/s1062739119045879.

Zhang, H., Wang, Z., Zheng, Y., Duan, P. and Ding, S. (2012), "Study on tri-axial creep experiment and constitutive relation of different rock salt", *Safety Sci.*, **50**(4), 801-805. https://doi.org/10.1016/j.ssci.2011.08.030.

Zhao, B.Y., Huang, T.Z., Liu, D.Y., Liu, Y., Wang, X.P., Liu, S. and Yu, G.B. (2019), "Study on the mechanical properties test and constitutive model of rock salt", *Geomech. Eng.*, **18**(3), 291-298. https://doi.org/10.12989/gae.2019.18.3.291.

Zhao, M. and Koves, W. (2012), "Isochronous stress-strain method with general state of stress and variable loading conditions for creep evaluation", *J. Pressure Vessel Technol.*, **134**(5), 051205. https://doi.org/10.1115/1.4007038.

Zahoor, M. and Puri, S. (2018), "Non-local continuum ductile damage model for rocks under high pressure and high temperature (HPHT)", *J. Petrol. Sci. Eng.*, **170**, 655-663. https://doi.org/10.1016/j.petrol.2018.06.090.

Zuo, Y.Y., Han, H., Hu, H., Luo, S.Y., Zhang, Y. and Chen, X.M. (2018), "Visco-elastic–Plastic creep constitutive relation of tunnels in soft schist", *Geotech. Geol. Eng.*, **36**(1), 389-400. https://doi.org/10.1007/s10706-017-0333-6.

CC